

ORIGINAL ARTICLE

Identification of an IDO1-based immune classifier for survival prediction of upper tract urothelial carcinoma

Wenlong Zhong^{1,2,3}  | Meng Yang⁴ | Sida Cheng⁵ | Weibin Hou⁶ | Bo Wang^{1,2,3} | Junyu Chen^{1,2,3} | Hao Yu^{1,2,3} | Yi Ouyang^{1,2,3} | Xiaofei Wang^{1,2,3} | Ziwei Ou^{1,2,3} | Peiqi Xu⁴ | Xuesong Li⁵ | Liqun Zhou⁵ | Jian Huang^{1,2,3} | Chunhui Wang⁴ | Tianxin Lin^{1,2,3,7}

¹Department of Urology, Sun Yat-sen Memorial Hospital, Sun Yat-sen (Zhongshan) University, Guangzhou, China

²Guangdong Provincial Key Laboratory of Malignant Tumor Epigenetics and Gene Regulation, Sun Yat-Sen Memorial Hospital, Sun Yat-Sen University, Guangzhou, China

³Guangdong Provincial Clinical Research Center for Urological Diseases, Guangzhou, China

⁴Department of Urology, Yan'an Hospital, Kunming Medical University, Kunming, China

⁵Department of Urology, Peking University First Hospital, Beijing, China

⁶Department of Urology, The Third Xiangya Hospital, Central South University, Changsha, China

⁷Kashgar Prefecture First People's Hospital of Kashi, Xinjiang, China

Correspondence

Chunhui Wang, Department of Urology, Yan'an Hospital of Kunming City, Kunming Medical University, Kunming, China.
Email: 13211604155@163.com

Tianxin Lin, Department of Urology, Sun Yat-sen Memorial Hospital, Sun Yat-sen (Zhongshan) University, Guangzhou 510120, China.
Email: lintx@mail.sysu.edu.cn

Funding information

This study was supported by the National Key Research and Development Program of China (no. 2018YFA0902803); the National Natural Science Foundation of China (no. 81902586, 81825016, 81961128027, 81772719 and 81772728); Guangdong Basic and Applied Basic Research Foundation (2020A1515011312); The Key Areas Research and Development Program of Guangdong (no. 2018B010109006);

Abstract

The limited response rate of immunotherapy in upper tract urothelial carcinoma (UTUC) might be attributed to additional immunosuppressive mechanisms in vivo. As a promising immune checkpoint target, the expression and prognostic role of indoleamine 2,3-dioxygenase 1 (IDO1) in UTUC remains unknown. In this study, the expression and prognostic value of IDO1 was analyzed in 251 patients from 3 independent cohorts. The least absolute shrinkage and selection operator (LASSO) Cox regression model was used to construct an IDO1-based immune classifier and external validation was performed to further validate the classifier. RNA sequencing and immunofluorescence were used to explore the immune contexture of different risk groups stratified by classifier. We found that high IDO1 expression on tumor cells (TC) indicated a poorer overall survival and disease-free survival in all cohorts. Patients with high expression of IDO1 TC possessed increased infiltration of CD4⁺, CD8⁺ and Foxp3⁺ T cells. An immune classifier based on intratumoral CD8⁺ lymphocytes, IDO1 TC, and stromal PD-L1 expression status was developed, with its area under the

Abbreviations: AUCs, area under the curves; BTLA, B and T lymphocyte associated; CK, cytokeratin; CTLA4, cytotoxic T-lymphocyte-associated protein-4; DFS, disease-free survival; FDR, false discovery rate; G1TR, glucocorticoid-induced tumor necrosis factor receptor; GSEA, gene set enrichment analysis; ICK, immune checkpoints; IC, immune cells; IDO1, indoleamine 2,3-dioxygenase 1; IF, immunofluorescence; IHC, immunohistochemistry; KYN, kynurenine; LAG3, lymphocyte activation gene-3; LASSO, least absolute shrinkage and selection operator; ORR, objective response rate; OS, overall survival; PD1, programmed cell death 1; PD-L1, programmed cell death-1 ligand; PKUFH, Peking University First Hospital; RNU, radical nephroureterectomy; ROC, receiver operating characteristic; ST, stromal infiltrating lymphocytes; SYSH, Sun Yat-sen Memorial Hospital; TC, tumor cells; TIGIT, T cell immunoreceptor with Ig and ITIM domains; TIL, tumor-infiltrating lymphocytes; TIM3, T cell immunoglobulin domain and mucin domain-3; TME, tumor microenvironment; UC, urothelial carcinoma; UCB, urothelial carcinoma of the bladder; UTUC, upper tract urothelial carcinoma; VISTA, V-set immunoregulatory receptor.

This is an open access article under the terms of the Creative Commons Attribution-NonCommercial License, which permits use, distribution and reproduction in any medium, provided the original work is properly cited and is not used for commercial purposes.

© 2021 The Authors. *Cancer Science* published by John Wiley & Sons Australia, Ltd on behalf of Japanese Cancer Association.

the Science and Technology Planning Project of Guangdong Province (no. 2017B020227007); Project Supported by Guangdong Province Higher Vocational Colleges & Schools Pearl River Scholar Funded Scheme (for Tianxin Lin); Guangdong Provincial Clinical Research Center for Urological Diseases (no. 2020B1111170006)

curves (AUCs) values for overall survival at 5 y being 0.79 (95% confidence interval [CI] 0.65–0.93) in the discovery cohort, 0.75 (95% CI 0.58–0.92) and 0.78 (95% CI 0.65–0.92) in the internal and external validation cohorts, respectively. The high-risk group stratified by the immune classifier was associated with immunosuppressive contexture, accompanied by enhanced CD8⁺ T cells exhaustion patterns. Our IDO1-based immune classifier can provide a superior accuracy for survival prediction and lead to individual stratification of UTUC immune subtypes.

KEYWORDS

CD8, immune classifier, indoleamine 2,3-dioxygenase 1, PD-L1, upper tract urothelial carcinoma

1 | INTRODUCTION

UTUC is a relatively rare malignancy, comprising only 5%–10% of UCs.^{1,2} Sharing similar biological and pathological characteristics with UCB, UTUC is more aggressive than UCB, with 60% of UTUC initially diagnosed as muscle-invasive tumors, compared with 15%–25% of UCB.³ Clinically, RNU with bladder cuff excision remains the gold standard treatment for UTUC. Accumulating evidence demonstrates that neoadjuvant or adjuvant chemotherapy can contribute to prolonged survival in patients with high-risk UTUC.^{4,5} However, despite these multidisciplinary treatments, the 5-y OS is less than 40% among cases of invasive disease.⁶

In the past decades, cancer immunotherapy targeting immune checkpoints has exhibited potential as a treatment strategy for several malignancies.⁷ Notably, treatment against the PD-L1/PD1 axis has been the first- or second-line treatment for selected patients with advanced or metastatic UC.^{8,9} Previous studies have demonstrated that the ORR of UTUC seems higher than that of UCB.¹⁰ However, only 21%–39% of patients can benefit from this treatment.¹¹ Additional immunosuppressive mechanisms might exist in patients with UTUC.

As a promising candidate target for immunotherapy, IDO1 can inhibit the proliferation and activation of T cells or NK cells by metabolizing the essential amino acid tryptophan into KYN, thereby participating in shaping the suppressive immune environment.¹² In

concert with the PD-L1/PD1 pathway, IDO1 is upregulated across different types of malignancy and therefore contributes to the negative regulation of the tumor-associated immune nature.^{13,14} Moreover, IDO1 expression may increase after anti-PD1 immunotherapy, suggesting that IDO1 represents a compensatory inhibitory pathway for immune escape.¹⁵ Small-sample-size retrospective studies on UC have suggested that IDO1 expression inversely affects the oncologic outcomes of UCB.¹⁶ To our knowledge, due to the relative rarity of UTUC, few studies have attempted to explore the expression and prognostic role of IDO1 in UTUC.

In the current study, we investigated the expression pattern and prognostic role of IDO1 in UTUC using 3 independent cohorts. In addition, we developed and validated an IDO1-based immune classifier, which could provide additional prognostic information and introduce personalized treatment for UTUC.

2 | MATERIALS AND METHODS

2.1 | Study population

The design of our study is presented in Figure 1. This study includes 251 consecutive patients with UTUC who underwent RNU. Patients with distant metastasis at diagnosis, concomitant with other malignant diseases, incomplete clinical information, missing pathological

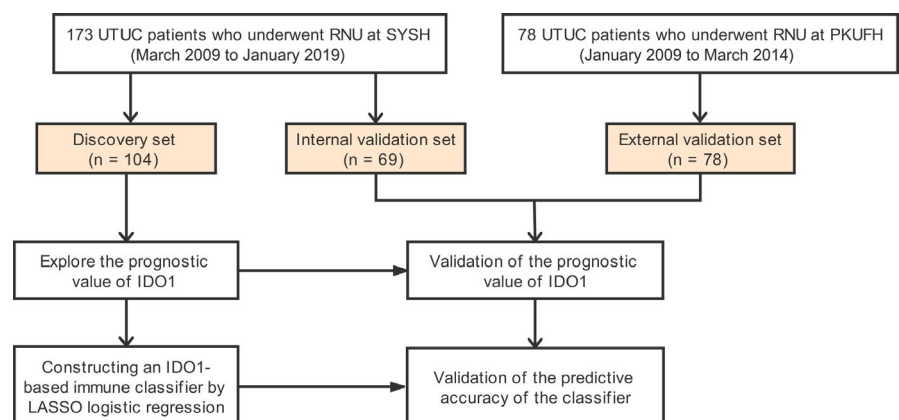


FIGURE 1 Design of the study. PKUFH, Peking University First Hospital; SYSH, Sun Yat-sen Memorial Hospital

tissue sections, or unscorable tissue sections and patients lost to follow-up were excluded from this study. Here, 173 consecutive patients at Sun Yat-sen Memorial Hospital from March 2009 to January 2019 were divided randomly into the discovery cohort ($n = 104$) and the internal validation cohort ($n = 69$). The 78 patients at Peking University First Hospital from January 2009 to March 2014 were set as an external validation cohort.

Clinicopathological data, including gender, age and tumor characteristics were collected. Pathological staging was determined in accordance with the tumor-node-metastasis staging system indicated in the 7th edition of the American Joint Committee on Cancer, and tumor grade was assessed under the 2004 World Health Organization classification. The primary endpoint of this study was OS, which was defined as the period from the date of surgery to death. The secondary endpoint was DFS, which was measured from the date of surgery to the date of cancer progression or death. Patients who were alive without documented clinical/radiographic disease recurrence were censored on the date of the last follow-up. This retrospective analysis was approved by the ethics committee of Sun Yat-sen Memorial Hospital and Peking University First Hospital, and written informed consent was obtained from each enrolled patient.

2.2 | Immunohistochemistry

Formalin-fixed paraffin-embedded tissue was sliced into 4- μ m sections, and IHC was conducted as previously described.¹⁷ After deparaffinization, endogenous peroxidase inactivation, rehydration, antigen retrieval, and blocking non-specific binding in IHC, the sections were incubated using primary antibodies against human IDO1 (1:400, Clone D5J4E, Cell Signaling Technology), PD-L1 (1:400, Clone SP142, Spring Bioscience), CD4 (1:400, Clone 23, Sino Biological Inc), CD8 (1:400, Clone D8A8Y, Cell Signaling Technology), and Foxp3 (1:100, Clone 236A/E7, Abcam), KYN (1:50, Clone 11F9, Santa Cruz). Following the incubation of the corresponding secondary antibody, the sections were visualized using 3,3'-diaminobenzidine tetrahydrochloride with the Envision System (Dako) and hematoxylin counterstain.

2.3 | Evaluation of immunohistochemical staining

The tissue sections were examined by 3 independent pathologists blinded to the clinicopathological and survival data. The specimens were evaluated for PD-L1 and IDO1 expression in TC and IC. The IDO1 expression levels were assigned the following scores: (0, no expression; 1, weak expression; 2, moderate expression; or 3, strong expression). The percentage of positive cells (0%-100%) was determined using the following formula: "expression level \times proportion of stained cells" ranging from 0 to 3. IDO1 staining in TC and IC were also evaluated separately; if staining area was ≥ 0.01 , positive staining was considered. The percentages of PD-L1⁺ in TC or IC were

estimated and were regarded as negative or positive if they were $<1\%$ or $\geq 1\%$ in TC, or if they were $<10\%$ or $\geq 10\%$ in IC, respectively. The immunoreactivity of KYN was semiquantitatively estimated and was graded as 0 (no expression), 1 (weak expression), 2 (moderate expression), or 3 (strong expression). The tumor samples were considered competent for KYN production when the IHC score was ≥ 1 . The density levels of CD4⁺, CD8⁺, and Foxp3⁺ TILs were measured in 5 representative high-power fields for each specimen ($\times 400$ magnification, 0.07 mm² per field). For the subsequent statistical analyses, the expression status of IDO1, PD-L1, CD4, CD8, and Foxp3 were recorded as dichotomous (high vs low) variable using X-tile software to calculate the optimal cutoff (Yale University, USA).

2.4 | Multiplexed immunofluorescence

Multiplexed IF was performed using OPAL-4-color reagents (Perkin-Elmer) in accordance with the instruction provided by the manufacturer. Antigen retrieval was conducted by immersing the tissue sections in citrate buffer in a microwave oven. The sections were blocked with 5% bovine serum albumin and incubated with the first primary antibody: IDO1 (1:3000, Clone D5J4E, Cell Signaling Technology); PD-L1 (1:2000, Clone SP142, Spring Bioscience); CK (1:1000, Clone AE1/AE3, Zhongshan Golden Bridge Bio-technology); CD8 (1:2000, Clone D8A8Y, Cell Signaling Technology); TIM3 (1:500, Clone D5D5R, Cell Signaling Technology); LAG3 (1:1000, Clone D2G4O); PD1 (1:500, Clone EH33, Cell Signaling Technology); VISTA (1:2000, Clone D5L5T, Cell Signaling Technology). IF staining was performed for panel 1: TIM3, LAG3, and CD8; panel 2: PD1, VISTA, and CD8, and panel 3: IDO1, PD-L1 and cytokeratin (CK) on 3 serial slides. The sections were further incubated with the secondary antibody for another period of 30 min at room temperature. After being washed 3 times in Tris-buffered solution with Tween, the tissue sections were incubated with the Opal Working Solution to generate the Opal signal (10 min at room temperature). Microwave treatment was then performed, followed by the second marker staining. After the last microwave treatment, the slides were stained with DAPI and then protected with coverslips. The IF staining was scanned using Phenochart 1.0.12 software. For quantification purposes, the infiltrated T cells per mm² were counted manually (average of 5 images at a $\times 400$ magnification).

2.5 | Transcript data

We retrospectively performed expression profiling of 29 available fresh tumor specimens from Peking University First Hospital (from January 2017 to December 2017) by high throughput sequencing. The backgrounds of the patients are shown in Table S3. The data were normalized and transformed into fragments per kilobase of exon model per million mapped fragments. We integrated CIBERSORT to estimate immune infiltration and hierarchical clustering to explore the association between tumor stratification and

immunosuppressive TME. Furthermore, we identified pathways that were upregulated and downregulated among groups by running a GSEA, significant pathways were identified with a strict cutoff of $P < .05$ and an FDR less than 0.25. The involved signatures and gene sets were defined from previous studies and evaluated as the primary expression levels of the related genes.¹⁷⁻¹⁹

2.6 | Statistical analysis

Correlations analyses were conducted using chi-square test for categorical variables and two-sided t test or Wilcoxon rank-sum test for continuous variables, as appropriate. Associations between parametric and nonparametric variables were evaluated using the Pearson correlation and the Spearman correlation, respectively. The log-rank test was used to compare survival differences based on immune marker expression. The Cox proportional-hazards model was used for multivariate analysis by including all statistically significant covariates ($P < .1$) from the univariate Cox model. The LASSO logistic regression model was used to construct an IDO1-based classifier and time-dependent ROC curves and AUCs at 5 y were generated to assess prognostic accuracy. All analyses were performed using the R programming language (v.3.5.0), GSEA (v.4.1.0) and SPSS Statistics 25 (SPSS Inc, IBM). A P -value $< .05$ was considered statistically significant.

3 | RESULTS

3.1 | Patient characteristics

The baseline clinicopathologic characteristics of the discovery and validation cohorts are summarized in Table 1. In total, 251 patients were enrolled into this study, with 104 patients in the discovery set, 69 patients in the internal validation set and 78 patients in the external validation set. For all patients, the median OS time was 34 mo (IQR: 15-60 mo), and the median DFS time was 24 mo (IQR: 11-51 mo). By the end of follow-up, 60 (23.9%) patients had died, and 100 (39.8%) patients had experienced disease progression. As shown, IDO1 was detected in both TC and IC with a predominant cytoplasmic staining pattern (Figure 2A-D). Overall, 90 patients (35.8%) presented with IDO1 expression in TC, whereas 204 patients (81.2%) presented with IDO1 expression in IC.

3.2 | IDO1 expression predicts poor clinical outcomes in patients with UTUC

We subsequently explored the prognostic value of IDO1 expression. We applied Kaplan-Meier curves and the log-rank test stratified by IDO1 TC and IC expression. By using X-tile software, the IDO1 expression pattern was determined as high if staining score >0.3 or low if staining score ≤ 0.3 in TC; the pattern was considered high if staining score >0.8 or low if staining score ≤ 0.8 in IC. In

the discovery cohort, higher expression of IDO1 TC was associated with worse OS ($P = .003$) and DFS ($P = .013$) (Figure 3A). However, no significant differences in OS and DFS were found between high and low expression groups of IDO1 IC (Figure 3B). Similar results were confirmed in the internal and external validation cohorts (Figure S1). Moreover, multivariate analysis indicated that high IDO1 TC expression was an independent prognostic factor for OS in the discovery set (HR = 2.51, 95% CI: 1.15-5.50; $P = .022$), the internal validation set (HR = 4.48, 95% CI: 1.68-11.99; $P = .003$), and the external validation set (HR = 10.07, 95% CI: 2.74-36.97; $P = .001$; Tables 2, S1, S2). When stratified by clinical factors (age, sex, tumor location, tumor size, and TNM stage) for subgroup analysis, IDO1 TC expression remained a clinically and statistically significant prognostic indicator for predicting OS (Figure S2). Therefore, these findings suggested that high IDO1 TC expression can potentially contribute to the progression and poor prognosis of UTUC.

3.3 | IDO1 expression was associated with T cells infiltration in UTUC

To explain the prognostic value of IDO1, we further evaluated the potential effect of IDO1 TC on immune contexture of UTUC. Firstly, we assessed the density of IC, including the CD4⁺, CD8⁺, and Foxp3⁺ T cells between the groups with high and low IDO1 TC expression levels. With regard to TIL, the patients with high IDO1 TC expression exhibited higher infiltration of Foxp3⁺ Tregs ($P < .001$), CD8⁺ T cells ($P = .004$), CD4⁺ T cells ($P = .044$), as well as a higher Foxp3⁺/CD8⁺ ratio ($P = .001$) (Figure 4A). Subgroup analysis based on CD8⁺ TIL revealed that IDO1 TC expression was associated with poor prognosis in the CD8 TIL-high subgroup, whereas no difference was observed in the CD8 TIL-low group ($P = .003$, 0.24, respectively; Figure 4B-D). Then, we found that the patients with high IDO1 TC expression exhibited higher KYN expression levels ($P = .032$; Figure S4A,B). Conclusively, these results indicated that IDO1 expression could potentially impact T cells infiltration in UTUC.

3.4 | IDO1 expression was irrelevant to the expression of PD-L1

Considering the potential of double-blockade of IDO1 and PD-L1, we measured the expression of PD-L1 in UTUC patients from the Sun Yat-sen Memorial Hospital cohorts. With cutoff values of 1% and 10% in TC and IC, the positive rates of PD-L1 expression were 42.2% and 39.3%, respectively. Notably, high positivity of PD-L1 expression in IC ($\geq 10\%$) was associated with poor OS and DFS, but no significant difference in survival was found between the groups with high and low PD-L1 expression levels in TC ($\geq 1\%$ or $<1\%$) (Figure 5A,B).

With regard to the co-expression pattern of IDO1 in TC and PD-L1 in IC, 72 patients (41.6%) were defined as both IDO1 and PD-L1 negative; only 25 patients (14.5%) exhibited positive expression of

| Variables | Total (n = 251) | Discovery set (n = 104) | Internal validation set (n = 69) | External validation set (n = 78) |
|----------------------|--------------------|----------------------------|--|--|
| Age (y, median, IQR) | 65 (58-73) | 65 (58-72) | 64 (57-75) | 66 (59-73) |
| < 65 | 123 (49.0%) | 52 (50.0%) | 35 (50.7%) | 36 (46.1%) |
| ≥ 65 | 128 (50.9%) | 52 (50.0%) | 34 (49.3%) | 42 (53.8%) |
| Gender | | | | |
| Female | 99 (39.4%) | 27 (26.0%) | 22 (31.9%) | 50 (64.1%) |
| Male | 152 (60.5%) | 77 (74.0%) | 47 (68.1%) | 28 (35.8%) |
| Side | | | | |
| Left | 129 (51.3%) | 55 (52.9%) | 38 (55.1%) | 36 (46.1%) |
| Right | 122 (48.6%) | 49 (47.1%) | 31 (44.9%) | 42 (53.8%) |
| Location | | | | |
| Pelvic | 149 (59.3%) | 60 (57.7%) | 41 (59.4%) | 48 (61.5%) |
| Ureter | 102 (40.6%) | 44 (42.3%) | 28 (40.6%) | 30 (38.4%) |
| Tumor size (cm) | | | | |
| < 3 | 100 (39.8%) | 36 (34.6%) | 18 (26.1%) | 42 (53.8%) |
| ≥ 3 | 151 (60.1%) | 68 (65.4%) | 51 (73.9%) | 36 (46.1%) |
| Multifocality | | | | |
| Unifocal | 199 (79.2%) | 87 (83.7%) | 58 (84.1%) | 54 (69.2%) |
| Multifocal | 52 (20.7%) | 17 (16.3%) | 11 (15.9%) | 24 (30.7%) |
| TNM stage | | | | |
| I-II | 136 (54.1%) | 61 (58.7%) | 31 (44.9%) | 44 (56.4%) |
| III-IV | 115 (45.8%) | 43 (41.3%) | 38 (55.1%) | 34 (43.5%) |
| Tumor grade | | | | |
| Low | 73 (29%) | 19 (18.3%) | 6 (8.7%) | 48 (61.5%) |
| High | 178 (70.9%) | 85 (81.7%) | 63 (91.3%) | 30 (38.4%) |
| Adjuvant therapy | | | | |
| No | 199 (79.2%) | 81 (77.9%) | 46 (66.7%) | 72 (92.3%) |
| Yes | 52 (20.7%) | 23 (22.1%) | 23 (33.3%) | 6 (7.6%) |
| IDO1 TC | | | | |
| Negative | 161 (64.1%) | 65 (62.5%) | 50 (72.5%) | 46 (58.9%) |
| Positive | 90 (35.8%) | 39 (37.5%) | 19 (27.5%) | 32 (41.0%) |
| IDO1 IC | | | | |
| Negative | 47 (18.7%) | 19 (18.3%) | 15 (21.7%) | 13 (16.6%) |
| Positive | 204 (81.2%) | 85 (81.7%) | 54 (78.3%) | 65 (83.3%) |

TABLE 1 The clinicopathologic characteristics of the discovery, internal, and external validation sets

Abbreviations: IC, immune cells; IDO1, indoleamine 2,3 dioxygenase 1; TC, tumor cells.

both IDO1 and PD-L1; no significant correlations between IDO1 TC and PD-L1 IC expression were found ($P = .51$; Figure 5C,D). Notably, 33 patients (19.1%) exhibited positive expression of IDO1 in the PD-L1-negative subgroup, which suggested the existence of distinct immune evasion pathways in UTUC (Figures 5E, S3).

3.5 | Construction and validation of the IDO1-based immune classifier

Accumulating evidence has suggested that the combined evaluation of immune checkpoints (ICK) and TIL could classify immune

phenotypes that provide risk stratification with enhanced accuracy, as well as predict the response to immunotherapy.²⁰⁻²² Therefore, we attempted to develop an immune classifier based on CD4, CD8, Foxp3, IDO1, and PD-L1 expression in UTUC. On the basis of the LASSO analysis in the discovery set, we identified 3 features as pivotal factors: CD8 TIL, PD-L1 IC, and IDO1 TC (Figure 6A,B). Then we calculated a risk score for each patient based on the immune signature status: risk score = $(0.1102876 \times \text{CD8 TIL status}) + (0.5486195 \times \text{PD-L1 IC status}) + (0.4498736 \times \text{IDO1 TC status})$.

All patients were further dichotomized into high-risk and low-risk groups using X-tile software. Kaplan-Meier survival analysis indicated a significant difference in OS between the discovery,

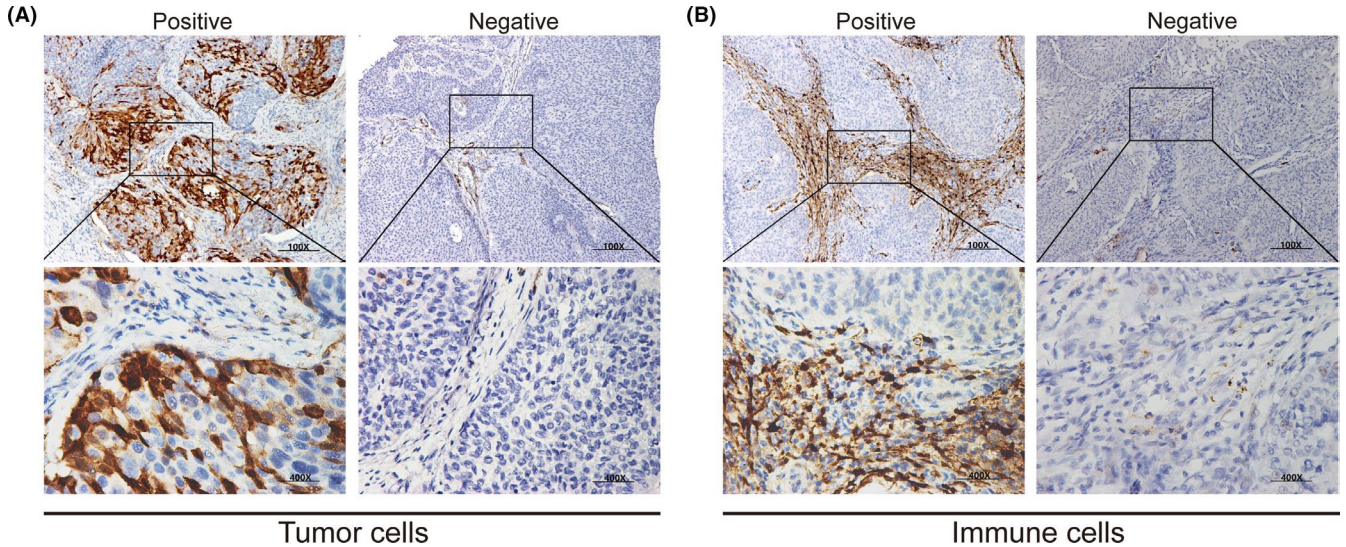


FIGURE 2 Immunohistochemical staining of IDO1 in UTUC. A, Positive and negative IDO1 expression on tumor cells is presented. B, Immune cell are positive or negative for IDO1. Photographs are shown at $\times 100$ or $\times 400$ magnification. IDO1, indoleamine 2,3-dioxygenase 1; UTUC, upper tract urothelial carcinoma

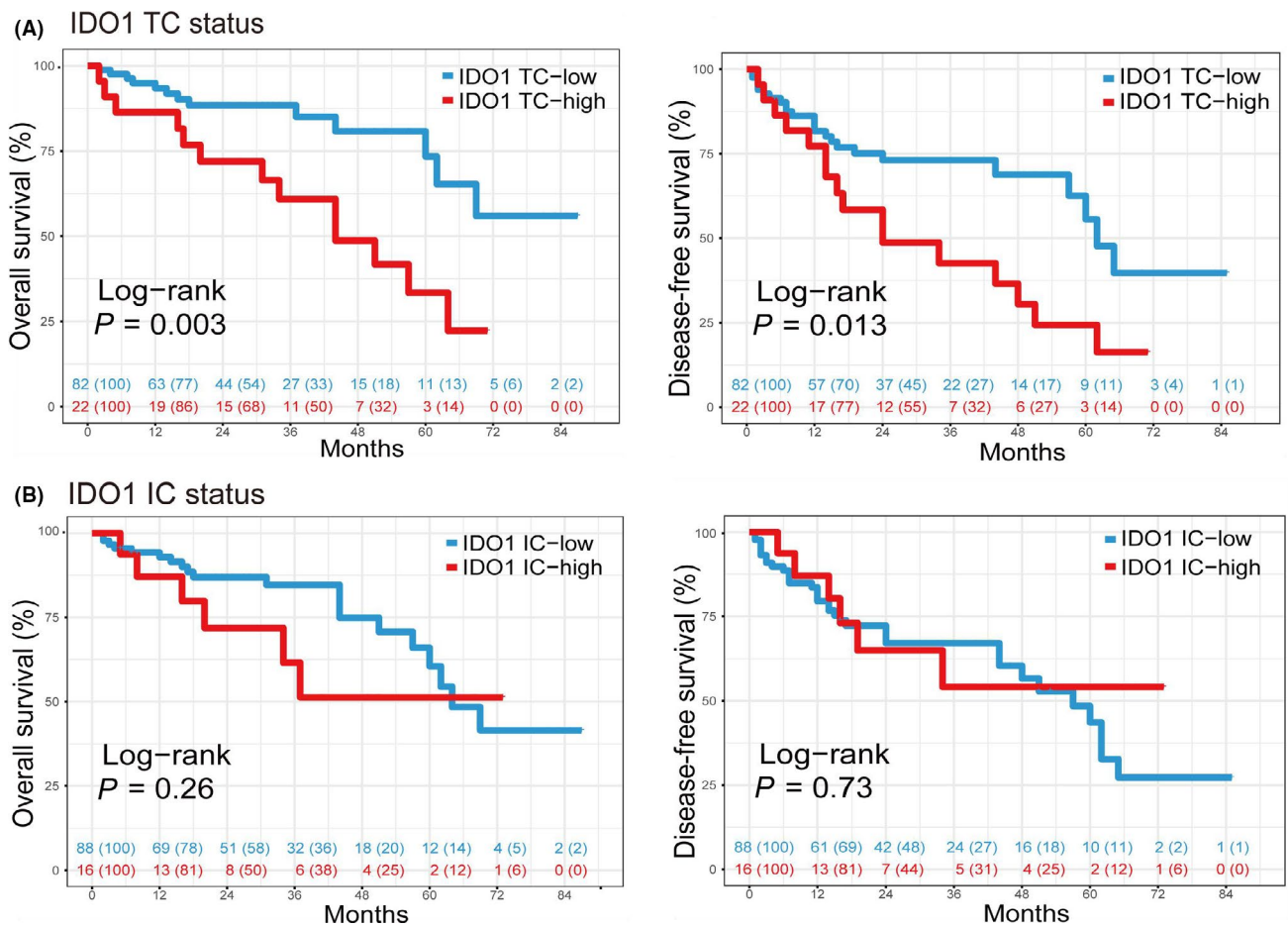


FIGURE 3 Tumor IDO1 expression predicts poorer prognosis in patients with UTUC. Kaplan-Meier curves of overall survival and disease-free survival according to expression of IDO1 TC (A) and IDO1 IC (B) expression status in the discovery cohort. Log-rank test was applied to Kaplan-Meier curves. IDO1, indoleamine 2,3-dioxygenase 1; UTUC, upper tract urothelial carcinoma; TC, tumor cells; IC, immune cells

TABLE 2 Univariate and multivariate analyses of prognostic factors associated with overall survival in discovery set

| Variables | Univariable analysis | | Multivariable analysis | |
|---|----------------------|-------------|------------------------|-------------|
| | HR (95% CI) | P-value | HR (95% CI) | P-value |
| Age (≥ 65 vs. < 65) | 0.96 (0.44-2.07) | .91 | | |
| Gender (male vs. female) | 0.93 (0.39-2.20) | .86 | | |
| Tumor location (ureter vs. pelvis) | 0.82 (0.37-1.81) | .63 | | |
| Side (right vs. left) | 1.45 (0.67-3.15) | .34 | | |
| Tumor size (≥ 3 cm vs. < 3 cm) | 0.79 (0.36-1.74) | .56 | | |
| Tumor multifocality (multifocal vs. unifocal) | 0.27 (0.06-1.15) | .08 | | |
| Pathologic stage (III-IV vs. I-II) | 4.15 (1.74-9.93) | .001 | 3.61 (1.50-8.73) | .004 |
| Pathologic grade (high vs. low) | 3.84 (0.90-16.32) | .07 | | |
| Adjuvant chemotherapy (yes vs. no) | 0.38 (0.09-1.62) | .19 | | |
| IDO1 (high vs. low) | 3.07 (1.41-6.67) | .005 | 2.51 (1.15-5.50) | .022 |

Abbreviations: CI, confidence interval; HR, hazard ratio.

The number in bold indicates statistically significant ($P < .05$).

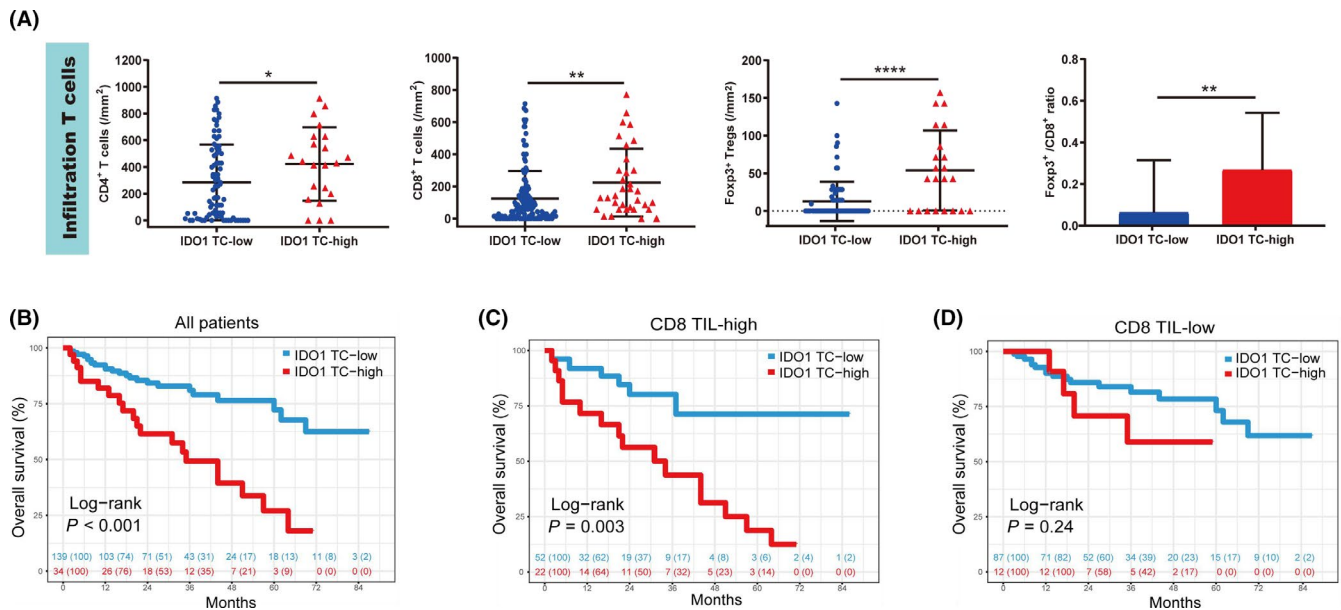


FIGURE 4 Tumor IDO1 expression was associated with immune contexture in UTUC. A, Relationship among densities of CD4⁺ T cells, CD8⁺ T cells, Foxp3⁺ Tregs and ratio of Foxp3⁺/CD8⁺ based on IDO1 TC expression levels using the unpaired *t* test. B-D, Kaplan-Meier curves of overall survival for IDO1 TC, and the combination of IDO1 TC with CD8⁺ T cells infiltration. Log-rank test was applied to the Kaplan-Meier curves. * $P < .05$; ** $P < .01$; *** $P < .001$. UTUC; upper tract urothelial carcinoma; IDO1, indoleamine 2,3-dioxygenase 1; TC, tumor cells; TIL, tumor-infiltrating lymphocytes

internal validation, and external validation cohorts ($P < .001$, $P = .04$, $P < .001$, respectively; Figure 6C-E). We used time-dependent ROC analysis to explore the prognostic discrimination capability of the signature. The AUCs for 5-y OS was 0.79 (95% CI 0.65-0.93) in discovery cohort, 0.75 (95% CI 0.58-0.92), and 0.78 (95% CI 0.65-0.92) in the internal and external validation cohorts, respectively. Moreover, the classifier exhibited a higher prognostic accuracy for 5-y OS than for the TNM stage and any other clinicopathological risk factors (Figure 6F-H). All aforementioned findings indicated that the immune classifier was also a powerful predictor for OS.

3.6 | The IDO1-based classifier reveals immunosuppressive contexture of UTUC

As the IDO1-based classifier might reflect the distinct immune contexture, we analyzed the distribution of IC infiltrates in different subgroups stratified by the classifier. The densities of CD8⁺ T cells and Tregs were significantly higher in the high-risk subgroup (low risk, $n = 14$; high risk, $n = 15$; Figure 7A).

Moreover, we hypothesized that high-risk tumors could counteract and impair the anti-tumor function of T cells by expressing ICK, and subsequently validated its determining capacity by

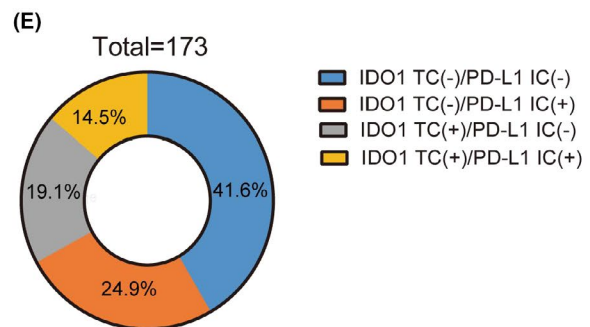
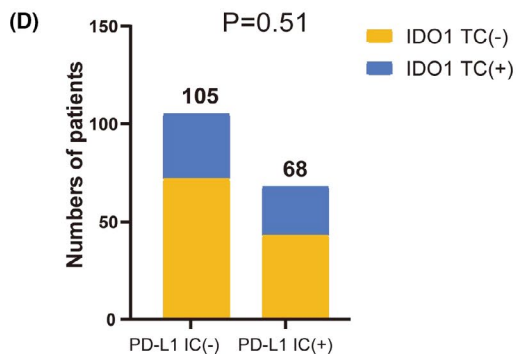
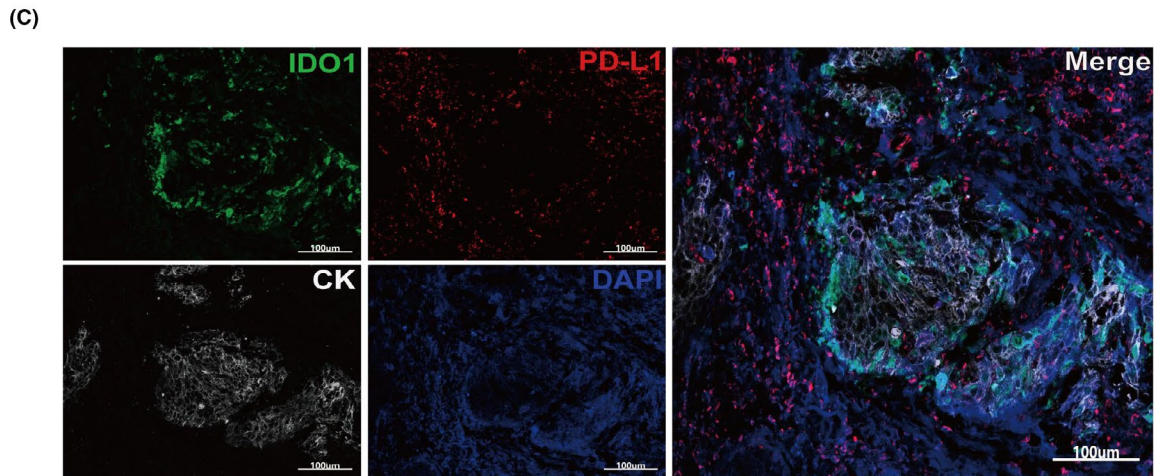
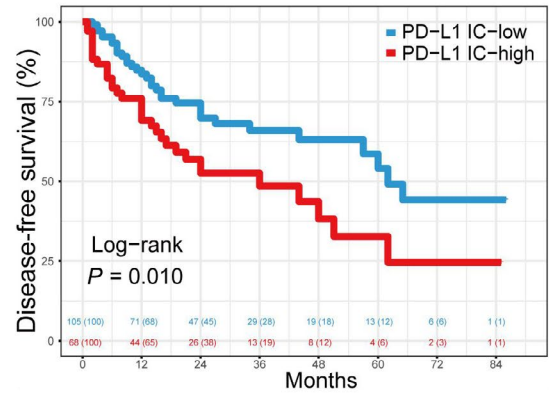
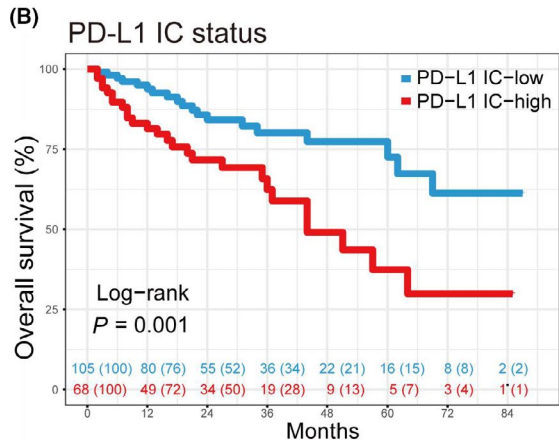
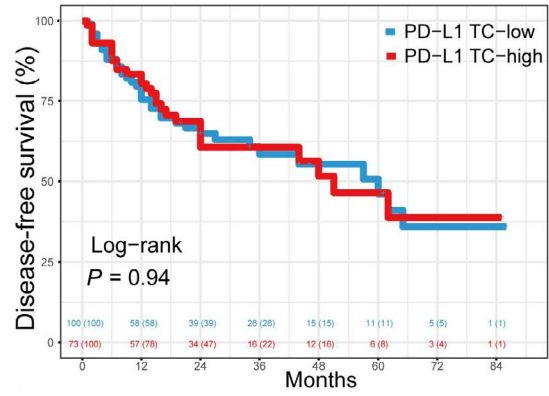
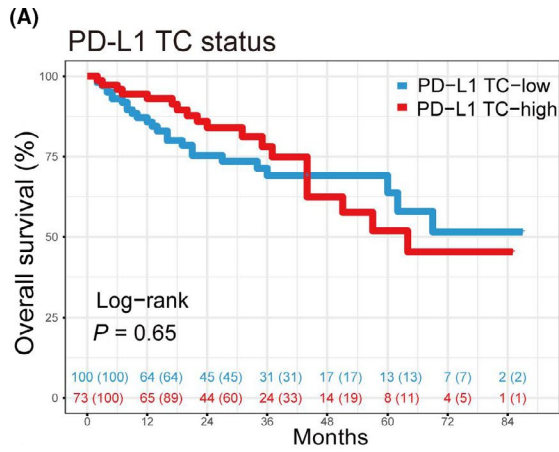


FIGURE 5 Tumor IDO1 expression was irrelevant to PD-L1. A, B, Kaplan-Meier curves of overall survival and disease-free survival in patients with PD-L1 TC and PD-L1 IC. C, Immunofluorescence staining for co-expression of IDO1 TC and PD-L1 IC (original magnification: $\times 100$). D, Statistical results of correlation between IDO1 TC and PD-L1 IC expression using the χ^2 test. E, Proportion analysis for IDO1 TC and PD-L1 IC in 4 different expression compartments. IDO1, indoleamine 2,3-dioxygenase 1; PD-L1, programmed cell death protein 1-ligand 1; TC, tumor cells; IC, immune cells

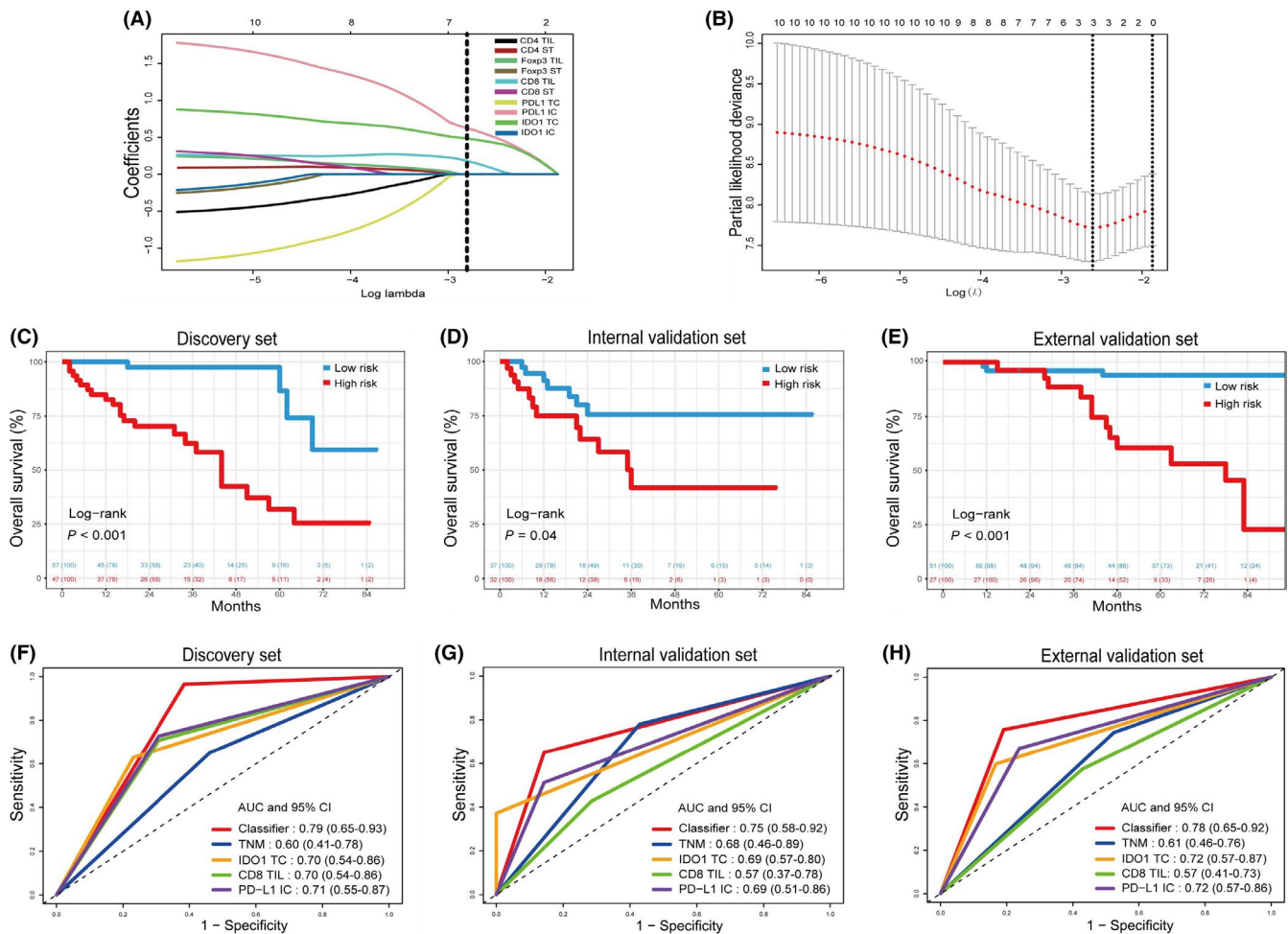


FIGURE 6 Construction and validation of the IDO1-based immune classifier. A, LASSO coefficient profiles of the 10 immune features. B, Selection of the tuning parameter (λ). The LASSO logistic regression model was used with penalty parameter tuning that was conducted by 10-fold cross-validation based on minimum criteria. C-E, Kaplan-Meier curves for overall survival between the immunoscore high and low-risk groups in different cohorts. F-H, Time-dependent ROC curves and AUCs at 5 y were used to assess the prognostic accuracy of the immune classifier compared with the TNM staging and immune signatures alone in different cohorts. AUCs, area under the curves; IC, immune cells; LASSO, least absolute shrinkage and selection operator; ROC, receiver operating characteristic; ST, stromal infiltrating lymphocytes; TC, tumor cells; TIL, tumor-infiltrating lymphocytes

hierarchical clustering. The transcript data confirmed that T cells that infiltrated into the high-risk subgroup presented an exhausted phenotype with elevated expression levels of PD1, VISTA, CTLA-4, TIM3, LAG3, TIGIT, BTLA, and GITR (Figure 7B). Using multiplexed immunofluorescence analysis, we further confirmed that patients in the high-risk group possessed higher infiltration of exhausted CD8⁺ T cells (TIM3⁺CD8⁺ T cells: $P = .006$; LAG3⁺CD8⁺ T cells: $P = .036$; PD1⁺CD8⁺ T cells: $P < .001$; and VISTA⁺CD8⁺ T cells: $P = .023$; Figure 7C,D). Given these findings, we performed GSEA using our transcript data. Consistently, GSEA with gene sets featuring exhausted CD8⁺ T cells and Tregs showed that these genes were

markedly overrepresented in the high-risk group for UTUC ($P < .001$, $P = .016$, respectively; Figure 7E).

4 | DISCUSSION

In this study, we comprehensively analyzed the prognostic value of IDO1 in 3 independent cohorts. Our data emphasized that IDO1 TC expression was associated with a poor prognosis for UTUC. We also developed and validated an IDO1-based immune classifier, which could reflect the immune contexture and provide improved

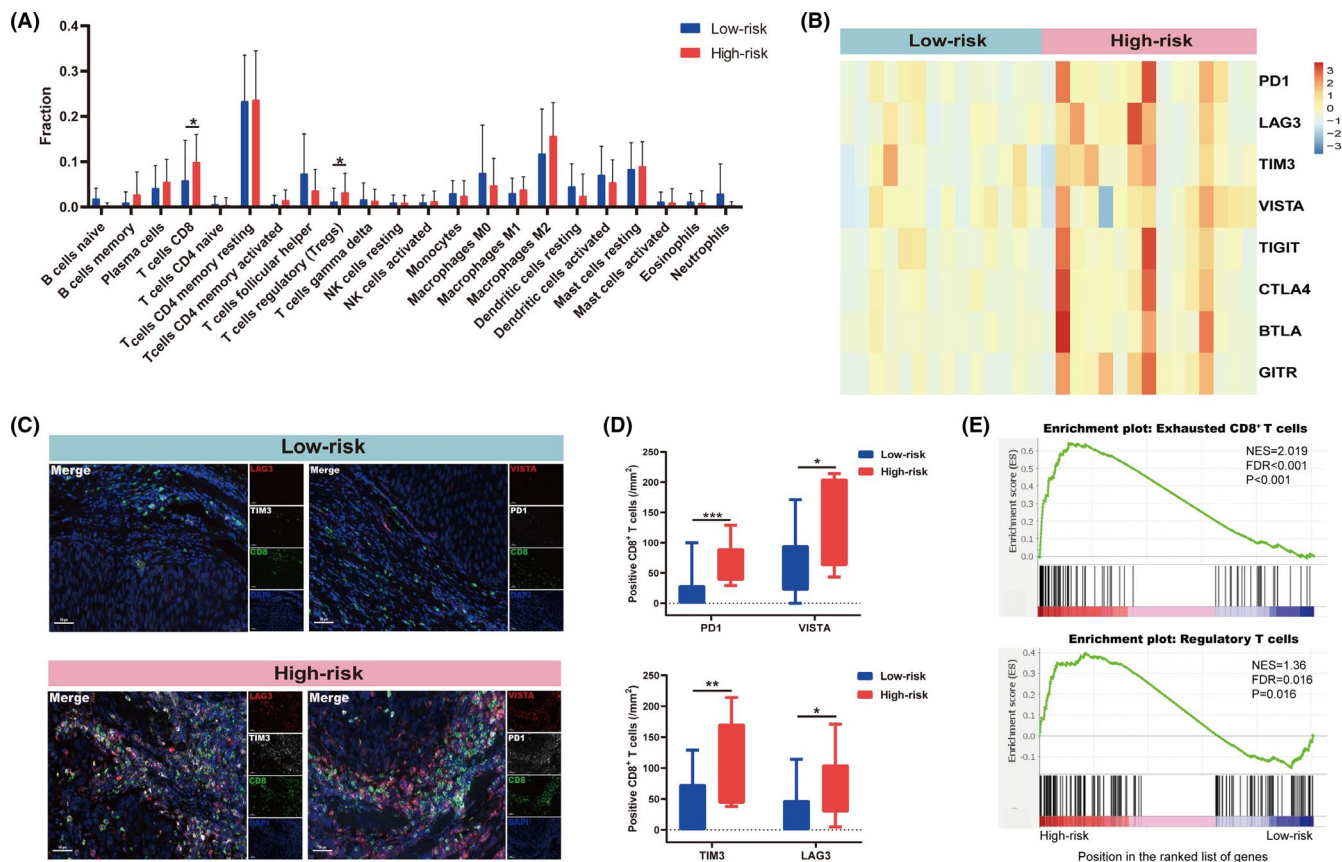


FIGURE 7 The IDO1-based immune classifier reflects different immune contexture between UTUC tumors. A, Densities of immune cells infiltration in low-risk ($n = 14$) and high-risk ($n = 15$) subgroups. B, Heatmap shows the percentages of ICK according to the stratification of our immune classifier. C, Representative multiplexed immunofluorescence images show different expression patterns of 4 common ICK in subgroups of UTUC (TIM3, LAG3, PD1, and VISTA; original magnification: $\times 200$). D, Using a t test to show the association between different groups and ICK expression on CD8⁺ T cells. E, Enrichment of genes related to exhausted CD8⁺ T cells and regulatory T cells in the high-risk group of UTUC. * $P < .05$; ** $P < .01$; *** $P < .001$. BTLA, B and T lymphocyte associated; CTLA-4, cytotoxic T-lymphocyte-associated protein-4; GITR, glucocorticoid-induced tumor necrosis factor receptor; IC, immune cells; ICK, immune checkpoints; IDO1, indoleamine 2,3-dioxygenase 1; LAG3, lymphocyte activation gene-3; PD1, programmed cell death 1; TC, tumor cells; TIGIT, T cell immunoreceptor with Ig and ITIM domains; TIL, tumor-infiltrating lymphocytes; TIM3, T cell immunoglobulin domain and mucin domain-3; UTUC, upper tract urothelial carcinoma; VISTA, V-set immunoregulatory receptor

prognostic prediction for UTUC. To our knowledge, this study is the first to investigate the prognostic role of IDO1 in UTUC and we developed the first immune-based prognostic model for UTUC.

IDO1 expression has been interrogated in multiple cancers and its role in tumor progression and metastasis has previously been reported. IDO1 could serve as a prognostic biomarker for poor oncologic outcomes,²³⁻²⁵ but opposite findings have been reported.^{26,27} Specifically, IDO1 can be expressed in both TC and IC, but the contribution of cell specificity to disease progression remains unclear. In the current study, we identified IDO1 TC expression as an independent risk factor for poor prognosis, but not IDO1 IC expression in UTUC. Accordingly, the role of IDO1 TC as a determinant may be strengthened, and it may be used as a therapeutic target for UTUC. In stark contrast, PD-L1 expression on IC is as important as, if not more important than, its expression on TC in terms of prognostic and ICK response prediction in cancers.²⁸⁻³⁰ This is also the case in UTUC as our data showed. As ICK on immune cells and tumor cells could independently attenuate anticancer immunity, this would be a

good reason for combining IDO1 on TC and PD-L1 on IC for therapeutic targeting and prognostic prediction in cancer.

The immunosuppressive role of IDO1 has been well established, considering that it can facilitate CD8⁺ T cell dysfunction and Treg differentiation, forming an immune-privileged position to facilitate tumor immune escape.^{23,31,32} A consistent finding in the current study was that IDO1 TC expression was strongly associated with increased infiltration of Foxp3⁺ Tregs and the Foxp3⁺/CD8⁺ ratio in UTUC. In addition, we found that IDO1 TC was significantly associated with increased CD8⁺ TIL, which is also indicated in other tumors.³³⁻³⁶ This phenomenon suggested a potential T-cell-mediated IDO1 enhancement in cancer. Our data also showed that IDO1 TC expression displayed significant prognostic value in the CD8⁺ TIL-high group instead of the CD8⁺ TIL-low group. These observations implied a tight connection between IDO1 TC and CD8⁺ TIL, which were the main targets of anti-PD1/PD-L1 therapies. IDO1 TC might be one of the crucial factors contributing to the adaptive resistance of ICK inhibitors in UTUC.

IDO1 has been currently evaluated as a dual blockage target in several solid tumors including UCB and non-small-cell lung cancer (NCT03832673, NCT02298153, and NCT03361865). Our preliminary data here emphasized that IDO1 expression on TC, together with PD-L1 expression on IC, were associated with immunoevasive TME in UTUC and therefore correlated with poor prognosis. Their irrelevant roles in tumor evasion and their distinct distributions in cell subsets provided a strong rationale for dual blockage of PD-L1 and IDO1 in patients with UTUC.

Previous studies have characterized the immune subtypes of tumors using PD-L1/PD1 expression and density of TIL, including the adaptive immune resistance, immunological ignorance, tolerance, and intrinsic induction.³⁷ The combination of IDO1 expression and CD8⁺ TIL has been found to act as a prognostic biomarker for cancer survival.^{20,38} Considering the irrelevant role of IDO1 expression in the PD-L1 axis, we developed an immune classifier including the infiltration of cytotoxic T cells, and IDO1 and PD-L1 expression to categorize patients with UTUC into high-risk and low-risk groups with large differences in OS. On the basis of the 3 immune variables, our immune classifier exhibited clear immunological relevance and robust prognostic power. This advantage could lead to an individualized risk stratification and treatment strategy for UTUC.

This study has several limitations. First, the retrospective nature of the study remained inevitably selection bias. Second, although the study was moderate in size for the rare disease, a larger sample size is needed to externally confirm the findings. Finally, the current immune classifier only included the CD8 TIL, IDO1 TC, and PD-L1 IC in UTUC. In the future, a more comprehensive classifier incorporating more immune cell types and other immune checkpoints might improve the prognostic value.

In conclusion, IDO1 TC expression created a profound immunosuppressive TME and therefore resulted in poor prognosis in UTUC. Moreover, we developed and validated an IDO1-based immune classifier, which might add prognostic value to the current clinical staging system. Together, our findings emphasized the potential role of IDO1 as a target for combined immunotherapy in UTUC.

ACKNOWLEDGMENTS

WZ, MY, SC, and WH performed experiments, statistical analysis and drafted of the manuscript. JC, HY, and Y-OY analyzed and interpretation of data. XW, ZO, and PX provided technical and material support. BW, XL, LZ, and JH provided study supervision and revised the manuscript. CW and TL designed the study. The authors would like to thank Dr. Guohui Huang from Department of Pathology, Sun Yat-sen Memorial Hospital for his assistance in IHC and IF score.

CONFLICT OF INTEREST

No potential competing interest was reported by the authors.

ETHICAL APPROVAL

All patients signed an informed consent before surgery that permitted the usage of resected tumors and clinical profiles in research,

under the condition of anonymity. The study was approved by the ethics committee of Sun Yat-sen Memorial Hospital and Peking University First Hospital.

DATA AVAILABILITY STATEMENT

The datasets used and/or analyzed during the current study are available from the corresponding author on reasonable request.

ORCID

Wenlong Zhong  <https://orcid.org/0000-0001-5343-4652>

REFERENCES

1. Roupêt M, Babjuk M, Burger M, et al. European association of urology guidelines on upper urinary tract urothelial carcinoma: 2020 Update. *Eur Urol*. 2021;79:62-79.
2. Bray F, Ferlay J, Soerjomataram I, et al. Global cancer statistics 2018: GLOBOCAN estimates of incidence and mortality worldwide for 36 cancers in 185 countries. *CA Cancer J Clin*. 2018;68:394-424.
3. Margulis V, Shariat SF, Matin SF, et al. Outcomes of radical nephroureterectomy: a series from the Upper Tract Urothelial Carcinoma Collaboration. *Cancer*. 2009;115:1224-1233.
4. Seisen T, Jindal T, Karabon P, et al. Efficacy of systemic chemotherapy plus radical nephroureterectomy for metastatic upper tract urothelial carcinoma. *Eur Urol*. 2017;71:714.
5. Matin SF, Margulis V, Kamat A, et al. Incidence of downstaging and complete remission after neoadjuvant chemotherapy for high-risk upper tract transitional cell carcinoma. *Cancer*. 2010;116:3127-3134.
6. Adibi M, Youssef R, Shariat SF, et al. Oncological outcomes after radical nephroureterectomy for upper tract urothelial carcinoma: Comparison over the three decades. *Int J Urol*. 2012;19:1060-1066.
7. Wang Y, Wang M, Wu HX, et al. Advancing to the era of cancer immunotherapy. *Cancer Commun (Lond)*. 2021;41(9):803-829.
8. Ning YM, Suzman D, Maher VE, et al. FDA approval summary: Atezolizumab for the treatment of patients with progressive advanced urothelial carcinoma after platinum-containing chemotherapy. *Oncologist*. 2017;22:743-749.
9. Vaughn DJ, Bellmunt J, Fradet Y, et al. Health-related quality-of-life analysis from KEYNOTE-045: a phase III study of Pembrolizumab versus chemotherapy for previously treated advanced urothelial cancer. *J Clin Oncol*. 2018;36:1579-1587.
10. Balar AV, Castellano D, O'Donnell PH, et al. First-line Pembrolizumab in cisplatin-ineligible patients with locally advanced and unresectable or metastatic urothelial cancer (KEYNOTE-052): a multicentre, single-arm, phase 2 study. *Lancet Oncol*. 2017;18:1483-1492.
11. Balar AV, Galsky MD, Rosenberg JE, et al. Atezolizumab as first-line treatment in cisplatin-ineligible patients with locally advanced and metastatic urothelial carcinoma: a single-arm, multicentre, phase 2 trial. *Lancet*. 2017;389:67-76.
12. Prendergast GC, Malachowski WJ, Mondal A, et al. Indoleamine 2,3-dioxygenase and its therapeutic inhibition in cancer. *Int Rev Cell Mol Biol*. 2018;336:175-203.
13. Takada K, Kohashi K, Shimokawa M, et al. Co-expression of IDO1 and PD-L1 in lung squamous cell carcinoma: potential targets of novel combination therapy. *Lung Cancer*. 2019;128:26-32.
14. Wainwright DA, Chang AL, Dey M, et al. Durable therapeutic efficacy utilizing combinatorial blockade against IDO, CTLA-4, and PD-L1 in mice with brain tumors. *Clin Cancer Res*. 2014;20:5290-5301.
15. Zhai L, Ladomersky E, Dostal CR, et al. Non-tumor cell IDO1 predominantly contributes to enzyme activity and response to CTLA-4/PD-L1 inhibition in mouse glioblastoma. *Brain Behav Immun*. 2017;62:24-29.

16. Zhang W, Zhang J, Zhang Z, et al. Overexpression of indoleamine 2,3-dioxygenase 1 promotes epithelial-mesenchymal transition by activation of the IL-6/STAT3/PD-L1 pathway in bladder cancer. *Transl Oncol*. 2019;12:485-492.
17. Zhong W, Wang B, Yu H, et al. Serum CCL27 predicts the response to bacillus calmette-guerin immunotherapy in non-muscle-invasive bladder cancer. *Oncoimmunology*. 2020;9:1776060.
18. Zheng C, Zheng L, Yoo JK, et al. Landscape of infiltrating T Cells in liver cancer revealed by single-cell sequencing. *Cell*. 2017;169:1342-1356.
19. FANTOM Consortium and the RIKEN PMI and CLST (DGT), Forrest AR, Kawaji H, et al. A promoter-level mammalian expression atlas. *Nature*. 2014;507:462-470.
20. Brown ZJ, Yu SJ, Heinrich B, et al. Indoleamine 2,3-dioxygenase provides adaptive resistance to immune checkpoint inhibitors in hepatocellular carcinoma. *Cancer Immunol Immunother*. 2018;67:1305-1315.
21. Duan J, Xie Y, Qu L, et al. A nomogram-based immunoprofile predicts overall survival for previously untreated patients with esophageal squamous cell carcinoma after esophagectomy. *J Immunother Cancer*. 2018;6:100.
22. Zou MX, Pan Y, Huang W, et al. A four-factor immune risk score signature predicts the clinical outcome of patients with spinal chordoma. *Clin Transl Med*. 2020;10:224-237.
23. Kiyozumi Y, Baba Y, Okadome K, et al. IDO1 expression is associated with immune tolerance and poor prognosis in patients with surgically resected esophageal cancer. *Ann Surg*. 2019;269:1101-1108.
24. Zhou QH, Han H, Lu JB, et al. Up-regulation of indoleamine 2,3-dioxygenase 1 (IDO1) expression and catalytic activity is associated with immunosuppression and poor prognosis in penile squamous cell carcinoma patients. *Cancer Commun (Lond)*. 2020;40:3-15.
25. Heeren AM, van Dijk I, Berry DRAI, et al. Indoleamine 2,3-dioxygenase expression pattern in the tumor microenvironment predicts clinical outcome in early stage cervical cancer. *Front Immunol*. 2018;9:1598.
26. Jacquemier J, Bertucci F, Finetti P, et al. High expression of indoleamine 2,3-dioxygenase in the tumour is associated with medullary features and favourable outcome in basal-like breast carcinoma. *Int J Cancer*. 2012;130:96-104.
27. Riesenberger R, Weiler C, Spring O, et al. Expression of indoleamine 2,3-dioxygenase in tumor endothelial cells correlates with long-term survival of patients with renal cell carcinoma. *Clin Cancer Res*. 2007;13:6993-7002.
28. Powles T, Eder JP, Fine GD, et al. MPDL3280A (anti-PD-L1) treatment leads to clinical activity in metastatic bladder cancer. *Nature*. 2014;515:558-562.
29. Rosenberg JE, Hoffman-Censits J, Powles T, et al. Atezolizumab in patients with locally advanced and metastatic urothelial carcinoma who have progressed following treatment with platinum-based chemotherapy: a single-arm, multicentre, phase 2 trial. *Lancet*. 2016;387:1909-1920.
30. Rodriguez-Barbosa JI, Azuma M, Zelinskyy G, et al. Critical role of PD-L1 expression on non-tumor cells rather than on tumor cells for effective anti-PD-L1 immunotherapy in a transplantable mouse hematopoietic tumor model. *Cancer Immunol Immunother*. 2020;69:1001-1014.
31. Munn DH, Mellor AL. IDO in the tumor microenvironment: inflammation, counter-regulation, and tolerance. *Trends Immunol*. 2016;37:193-207.
32. Baban B, Chandler PR, Sharma MD, et al. IDO activates regulatory T cells and blocks their conversion into Th17-like T cells. *J Immunol*. 2009;183:2475-2483.
33. Schollbach J, Kircher S, Wiegner A, et al. Prognostic value of tumour-infiltrating CD8+ lymphocytes in rectal cancer after neoadjuvant chemoradiation: is indoleamine-2,3-dioxygenase (IDO1) a friend or foe? *Cancer Immunol Immunother*. 2019;68:563-575.
34. Li S, Han X, Lyu N, et al. Mechanism and prognostic value of indoleamine 2,3-dioxygenase 1 expressed in hepatocellular carcinoma. *Cancer Sci*. 2018;109(12):3726-3736.
35. Zhang ML, Kem M, Mooradian MJ, et al. Differential expression of PD-L1 and IDO1 in association with the immune microenvironment in resected lung adenocarcinomas. *Mod Pathol*. 2019;32:511-523.
36. Zhai L, Ladomersky E, Lauing KL, et al. Infiltrating T cells increase IDO1 expression in glioblastoma and contribute to decreased patient survival. *Clin Cancer Res*. 2017;23:6650-6660.
37. Teng MW, Ngiow SF, Ribas A, et al. Classifying cancers based on T-cell infiltration and PD-L1. *Cancer Res*. 2015;75:2139-2145.
38. Zhou S, Yang H, Zhang J, et al. Changes in indoleamine 2,3-dioxygenase 1 expression and CD8+ tumor-infiltrating lymphocytes after neoadjuvant chemoradiation therapy and prognostic significance in esophageal squamous cell carcinoma. *Int J Radiat Oncol Biol Phys*. 2020;108:286-294.

SUPPORTING INFORMATION

Additional supporting information may be found in the online version of the article at the publisher's website.

How to cite this article: Zhong W, Yang M, Cheng S, et al. Identification of an IDO1-based immune classifier for survival prediction of upper tract urothelial carcinoma. *Cancer Sci*. 2022;113:852-863. doi:[10.1111/cas.15253](https://doi.org/10.1111/cas.15253)